Nonnucleosidic Base Surrogates: The Effect of 1,2-Disubstituted Phenanthrenes on DNA Duplex Stability

by **Damian Ackermann** and **Robert Häner***

Department of Chemistry and Biochemistry, University of Berne, Freiestrasse 3, CH-3012 Bern
(phone: +41 31 631 4382; e-mail: robert.haener@ioc.unibe.ch)

Phenanthrene-1,2-dimethanol was incorporated into oligodeoxynucleotides *via* formation of phosphodiester bonds (*cf. Scheme 1*). If placed at internal positions in a DNA duplex, a strong reduction of duplex stability is observed (*Table 1*). Terminal attachment of stretches of phenanthrene residues, however, leads to a substantial increase in stability. The stabilization is attributed to a cooperative interaction of the phenanthrene residues of the two strands rather than to dangling end effects. Chimeric oligomers containing a stretch of six phenanthrene residues show two separate transitions (*Table 2*): one arising from the denaturation of the DNA stem (observable by a hyperchromic effect at 260 nm) and a second one from the denaturation of the phenanthrene part (observable by temperature-dependant gel mobility assays). Based on these findings, a model of the chimeric hybrids is proposed, in which the phenanthrene residues stack in a zipper-like manner on top of the DNA base pairs without disrupting the B-form of the DNA stem (see *Fig. 7*).

1. Introduction. – Modified oligonucleotides have found widespread applications as diagnostic and research tools. Furthermore, the generation of defined molecular structures by using nucleic acid like building blocks is a research topic of increasing interest [1]. Among the many factors contributing to the formation and stabilization of secondary and tertiary structures in nucleic acids, aromatic stacking interactions [2] play a predominant role. The influence of nucleoside-linked aromatic and heteroaromatic base analogs on duplex stability and base pairing properties has been reported [3–9] and reviewed [10]. Furthermore, dangling nucleotides [11–13] or other terminal aromatic residues, such as quinolones [14], pyrene [15], and naphthalenediimides [15] may substantially increase the stability of a DNA duplex. Furthermore, it has been shown that the incorporation of aromatic building blocks *via* flexible, nonnucleosidic linkers into DNA gives rise to stable duplexes in which the nonnatural building blocks contribute to the duplex stability by aromatic stacking interactions [16–19]. Within the context of developing nonnucleosidic DNA-like building blocks, we investigated the 1,2-disubstituted phenanthrene building block shown in *Scheme 1*. Model studies suggested that this building block, which is amenable to oligomerization *via* phosphodiester-bond formation, should fit well into the right-handed helical structure of natural B-DNA. Here, we report the synthesis of the building block **1**, its incorporation into oligodeoxynucleotides, as well as its influence on the structure and stability of DNA.

2. Results and Discussion. – *2.1. Synthesis of the Phosphoramidite Building Block* **1.** At 130°, 1-ethenylnaphthalene (**2**) was treated with 2 equiv. of dimethyl ethynedicar-

Scheme 1. *Illustration of Oligo(phenanthrylmethyl phosphates)*

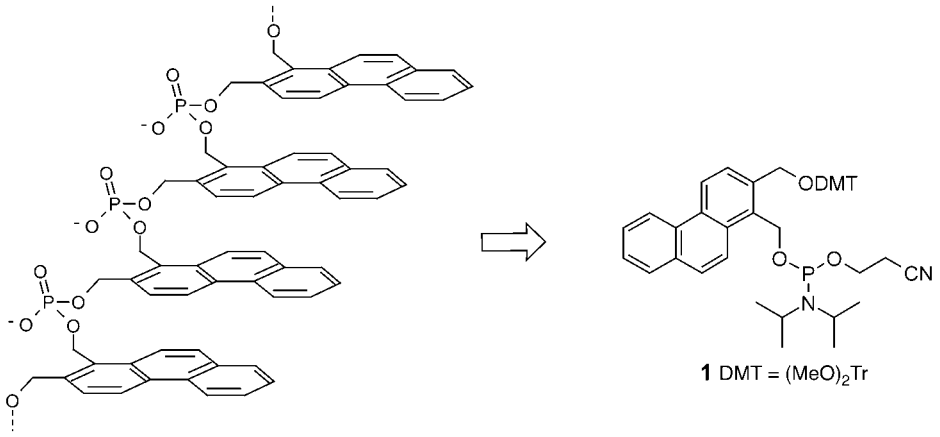

boxylate in *o*-xylene for 3 h [20] to give **3** in a moderate yield of 34% (*Scheme 2*). Reduction of diester **3** with $LiBH_4$ [21] followed by crystallization afforded the desired diol **4** in 34% yield. Reaction with 4,4′-dimethoxytrityl chloride ($(MeO)_2TrCl$) led to the formation of a 4 : 1 mixture of the two regioisomers **5** and **6**, which were separated by column chromatography. The correct assignment of the regioisomeric structures was achieved through nuclear *Overhauser* experiments (NOE, see *Exper. Part*) with the chloroacetate **7**, which was obtained by derivatization of **5**. Treatment of **5** with 2-cyanoethyl diisopropylphosphoramidochloridite gave the desired phosphoramidite **1**. Furthermore, **5** was immobilized on controlled-pore glass (CPG) according to the literature [22]. The solid support **8** was obtained with a loading density of 26 μmol/g (see *Exper. Part*).

2.2. *Synthesis and Purification of DNA/Phenanthrene Hybrid Oligomers.* The phosphoramidite **1** was incorporated into a series of different chimeric oligodeoxynucleotides (summarized in *Tables 1* and *2*). Incorporation of the modified building block proceeded without difficulties under the standard conditions used for automated oligonucleotide synthesis. Oligomers were assembled on commercial CPG solid supports except for **1b**, **1c**, **1f**, **1g**, **1h**, **1k**, and **1l**, which were synthesized on the solid support **8**. After removal from the support and deprotection of the oligomers (10M conc. aqueous ammonia, 55° for 16 h), the crude products where purified by HPLC. Sequences containing no or a single phenanthrene building block were purified on anion-exchange material. Purification of sequences containing two or more phenanthrene residues was possible only on reversed-phase stationary phase (see *Exper. Part*). After desalting, all compounds were characterized by ESI-MS and stored as stock solutions in H_2O.

2.3. *Thermal Denaturation Experiments.* The stability of the phenanthrene-modified DNA hybrid duplexes was analyzed by temperature-dependent UV spectroscopy. The samples were measured at 2 μM duplex concentration in a solution of 150 mM NaCl and 10 mM *Tris* · HCl in H_2O at pH 7.4. T_m Values were taken from the maximum of the first derivative of the melting curves. All UV melting curves of the duplexes listed in *Table 1* had a sigmoidal shape and showed one single transition. *Fig. 1* shows the denaturation

Scheme 2. *Synthesis of Phosphoramidite Building Block* **1** *and Solid Support* **8**

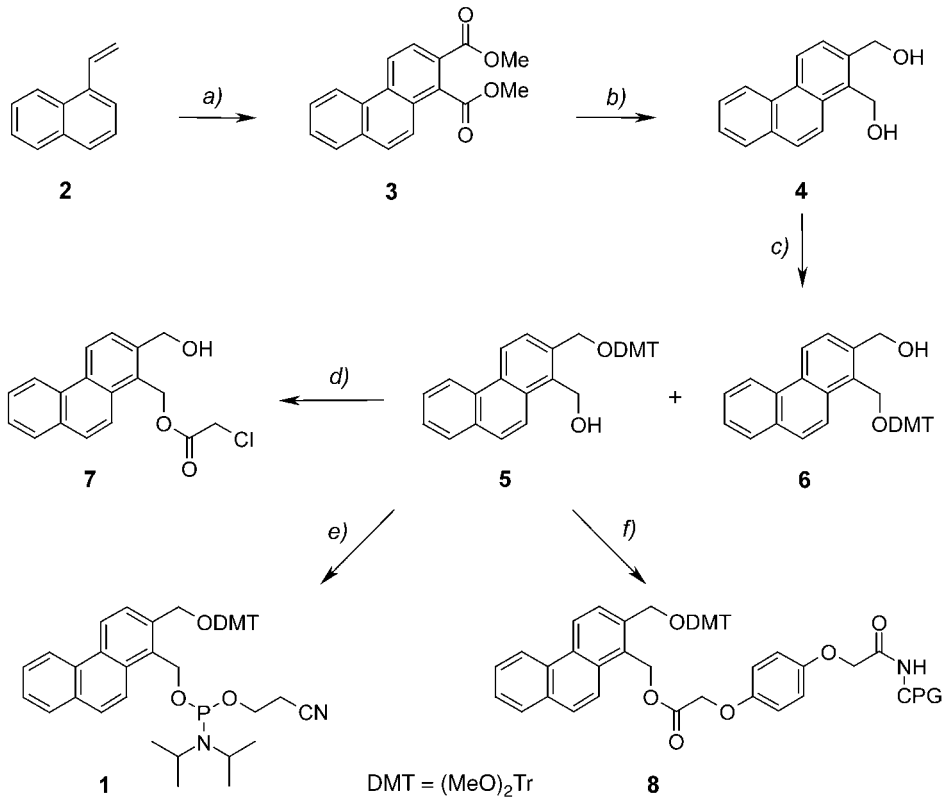

a) Dimethyl ethynedicarboxylate, *o*-xylene (=1,2-dimethylbenzene), 130°, 3 h, recryst.; 34%. *b*)$LibH_4$, MeOH, THF, reflux, 1 h; 34%. *c*) $(MeO)_2Tr$, Et_3N, pyridine, 17 h, r.t.; 42% (**5**), 8% (**6**). *d*) 1. Chloroacetatic anhydride, collidine (=2,4,6-trimethylpyridine), -ch_2Cl_2, r.t., 15 min; 2. HCOOH/THF/EtOH 50 : 35 : 15, 20 min, r.t.; 32%. *e*) $CIP^iPr_2N)OCH_2CH_2CN$, $^iPr_2NEt$, CH_2Cl_2, r.t., 30 min; 88%. *f*) 1. [1,4-phenylenebis(oxy)bis[acetic acid], BOP (=(1*H*-benzotriazol-1-yloxy)tris(dimethylamino)phosphonium hexafluorophosphate), $^iPr_2NEt$, DMAP (=*N*,*N*-dimethylpyridin-A-amine), pyridine, r.t., 1 h; 2. LCAA-GPG $^iPr_2NEt$, BOP, MeCN, r.t., 20 h; 3. Ac_2O, pyridine, r.t., 2 h; loading: 26 μmol/g.

curves for *Entries 1–5*. Furthermore, heating and cooling curves were superimposable for each duplex, which means that the melting and annealing processes are at equilibrium under the experimental conditions.

The T_m data show that replacement of terminal base pairs with building block **B** (*Table 1*, *Entries 2* and *3*) leads to an increase in the T_m (4.3 and 7.6° for one and three pairs of **B**, resp.). In contrast, introduction of **B** residues in the middle (*Entries 4* and *5*) results in a large decrease in duplex stability (−19.2 and −33.5°, resp.). Very similar trends were observed for duplexes where only one modified strand was paired with the complementary reference strand. One or three phenanthrene residues attached at the end of one strand have a small stabilizing or destabilizing effect (*Entries 6–8*). On the other hand, phenanthrene residues in the middle of the duplex (*Entries 9* and *10*) are not tolerated and, hence, lead to a severe destabilization. Thus, the data summarized in

Table 1. *Melting Temperatures of Phenanthrene-Containing DNA Duplexes*

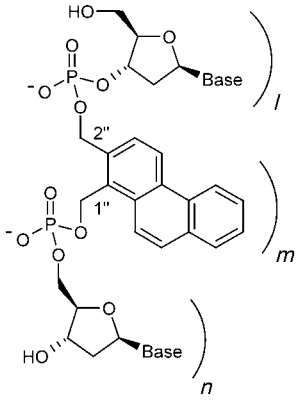

(DNA)$_l$-**B**$_m$-(DNA)$_n$

Entry	Duplex[a])		T_m [°][b])	ΔT_m [°]
1	**1a** · **2a**	5′ AGC TCG GTC ATC 3′ 3′ TCG AGC CAG TAG 5′	56.2	–
2	**1b** · **2b**	5′ AGC TCG GTC AT**B** 1″ 3′ TCG AGC CAG TA**B** 2″	60.5	4.3
3	**1c** · **2c**	5′ AGC TCG GTC **BBB** 1″ 3′ TCG AGC CAG **BBB** 2″	63.8	7.6
4	**1d** · **2d**	5′ AGC TCG **B**TC ATC 3′ 3′ TCG AGC **B**AG TAG 5′	37.0	– 19.2
5	**1e** · **2e**	5′ AGC T**BB B**TC ATC 3′ 3′ TCG A**BB B**AG TAG 5′	22.7	– 33.5
6	**1a** · **2b**	5′ AGC TCG GTC ATC 3′ 3′ TCG AGC CAG TA**B** 2″	57.3	1.1
7	**1b** · **2a**	5′ AGC TCG GTC AT**B** 1″ 3′ TCG AGC CAG TAG 5′	58.2	2.0
8	**1a** · **2c**	5′ AGC TCG GTC ATC 3′ 3′ TCG AGC CAG **BBB** 2″	55.4	– 0.8
9	**1a** · **2d**	5′ AGC TCG GTC ATC 3′ 3′ TCG AGC **B**AG TAG 5′	35.5	– 20.7
10	**1a** · **2e**	5′ AGC TCG GTC ATC 3′ 3′ TCG A**BB B**AG TAG 5′	< 5.0	< – 51.2

[a]) **B** denotes the nonnucleosidic phenanthrene residue derived from phosphoramidite **1** (see *Scheme 1*); 1″ or 2″ denotes linkage to CH_2O at C(1) or C(2), respectively, of the phenanthrene residue. [b]) Conditions for T_m measurements: 2 μM duplex conc., 150 mM NaCl, 10 mM *Tris* · HCl (pH 7.4); exper. error: ± 0.5°.

Table 1 allow the following conclusion: *i*) building block **B** leads to a strong decrease in DNA duplex stability if incorporated in the middle of the duplex stem, and *ii*) terminal attachment of **B** – either pairwise or a single opposite to a natural nucleotide – increases duplex stability.

2.4. *Effect of Terminal Phenanthrene Residues on Duplex Stability.* Based on these observations, we extended our studies to chimeric oligomers with terminally attached phenanthrene units of type **B** (see *Table 2*). All melting curves show a single transition, indicating a cooperative melting of the hybrids (*Fig. 2*). While the hybrids with one, two, and three phenanthrene pairs show no difference between the heating and cooling

Table 2. *Melting Temperatures of DNAs Containing Terminal Phenanthrene Residues*

Entry	Duplex[a])		T_m [°][b])	ΔT_m [°]
11	**1r**·**2r**	5′ AGC TCG 3′ 3′ TCG AGC 5′	20.3	–
12	**1f**·**2f**	5′ AGC TCG **B** 1″ 3′ TCG AGC **B** 2″	27.9	7.6
13	**1g**·**2g**	5′ AGC TCG **BB** 1″ 3′ TCG AGC **BB** 2″	36.9	16.6
14	**1h**·**2h**	5′ AGC TCG **BBB** 1″ 3′ TCG AGC **BBB** 2″	34.3	14.0
15	**1i**·**2i**	5′ AGC TCG **BBB B** 1″ 3′ TCG AGC **BBB B** 2″	36.2, 38.0[c])	15.9, 17.7[c])
16	**1k**·**2k**	5′ AGC TCG **BBB BB** 1″ 3′ TCG AGC **BBB BB** 2″	12.5, 30.4[c])	– 7.8, 10.1[c])
17	**1l**·**2l**	5′ AGC TCG **BBB BBB** 1″ 3′ TCG AGC **BBB BBB** 2″	29.6, 40.2[c])	9.3, 19.9[c])
18	**1f**·**2r**	5′ AGC TCG **B** 1″ 3′ TCG AGC 5′	25.6	5.3
19	**1g**·**2r**	5′ AGC TCG **BB** 1″ 3′ TCG AGC 5′	24.3	4.0
20	**1h**·**2r**	5′ AGC TCG **BBB** 1″ 3′ TCG AGC 5′	23.8	3.5
21	**1i**·**2r**	5′ AGC TCG **BBB B** 1″ 3′ TCG AGC 5′	n.o.	–
22	**1k**·**2r**	5′ AGC TCG **BBB BB** 1″ 3′ TCG AGC 5′	n.o.	–
23	**1l**·**2r**	5′ AGC TCG **BBB BBB** 1″ 3′ TCG AGC 5′	n.o.	–
24	**1r**·**2f**	5′ AGC TCG 3′ 3′ TCG AGC **B** 2″	34.3	14.0
25	**1r**·**2g**	5′ AGC TCG 3′ 3′ TCG AGC **BB** 2″	31.0	10.7
26	**1r**·**2h**	5′ AGC TCG 3′ 3′ TCG AGC **BBB** 2″	29.0	8.7
27	**1r**·**2i**	5′ AGC TCG 3′ 3′ TCG AGC **BBB B** 2″	27.1	6.8
28	**1r**·**2k**	5′ AGC TCG 3′ 3′ TCG AGC **BBB BB** 2″	25.7	5.4
29	**1r**·**2l**	5′ AGC TCG 3′ 3′ TCG AGC **BBB BBB** 2″	27.1	6.8

[a]) **B** denotes the nonnucleosidic phenanthrene residue derived from phosphoramidite **1** (see *Scheme 1*); 1″or 2″ denotes linkage to C(1) or C(2), respectively, of the phenanthrene residue. [b]) Conditions for T_m measurements: 2 μM duplex conc., 150 mM NaCl, 10 mM *Tris*·HCl (pH 7.4); n.o. = no transition observed. [c]) First value is taken from cooling ramp, second value from heating ramp (for cases, in which hysteresis was observed).

cycles, a slight hysteretic effect (*ca.* 2°) is observed with four phenanthrene pairs (*Entry 15*). This effect increases dramatically upon addition of further phenanthrene pairs. Thus, large hysteretic effects were observed with hybrids containing five and six phenanthrene pairs (*Entries 16* and *17*) even when small heating rates (0.2°/min, data not shown) were applied. The results of thermal denaturation studies are summarized in *Table 2*. The T_m data show that the attachment of terminal phenanthrene pairs results in a substantial increase in the melting temperature. Thus, the value gradually increases

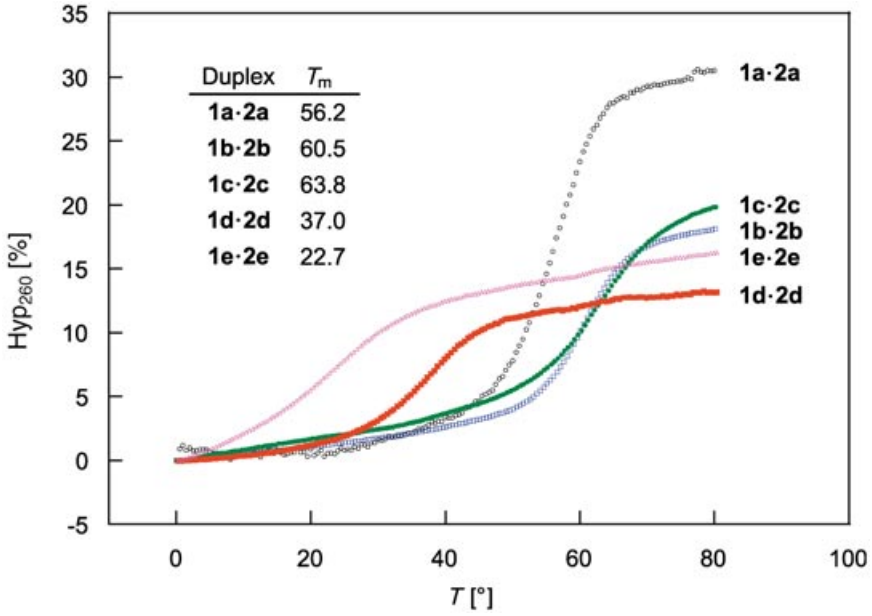

Fig. 1. *UV Melting curves of the duplexes* **1a** · **2a**, **1b** · **2b**, **1c** · **2c**, **1d** · **2d**, **1e** · **2e** (*Table 1*, *Entries 1–5*). Conditions: 2 μM duplex concentration, 150 mM NaCl, and 10 mM *Tris* · HCl in H_2O (pH 7.4); heating and cooling rate: 0.5°/min.

from 20.3° to 38.0° upon addition of up to four phenanthrene pairs. The determination of the T_m values for the hybrids with five and six phenanthrene pairs is complicated by the relatively slow kinetics of the denaturation/renaturation process resulting in the hysteretic effect mentioned above. In general, however, the trend indicates a leveling of the T_m values.

The positive effect on duplex stability by dangling nucleotides [11] or aromatic residues is well known [12][14]. It is possible that this – sometimes very large – effect is responsible for the stabilization we observed with the phenanthrene-containing duplexes. To further elucidate this question, we investigated the effect on duplex stability of dangling phenanthrene units on either of the two strands. The denaturation curves were measured under the same conditions as with the other oligomers. The results are given in *Table 2* (*Entries 18–29*). As expected, terminal attachment of phenanthrene residues leads to an increase in duplex stability. The 5′-linked residues (*Entries 24–29*) have a much more pronounced effect than the 3′-linked analogs (*Entries 18–23*). The largest stabilization results from a single aromatic residue. Upon addition of further dangling phenanthrene units, however, a steady reduction of T_m is observed in both series. With more than three phenanthrene residues at the 3′-end, no transition is observed anymore. The different trends are represented in *Fig. 3* showing the ΔT_m values as a function of the number of attached phenanthrene units, either as dangling residues or as phenanthrene pairs. The curves reveal that the stabilization resulting from one phenanthrene pair (blue curve) is less than the sum of the stabilizations by one 3′- and one 5′-dangling residues (red curve). Two, three, or four

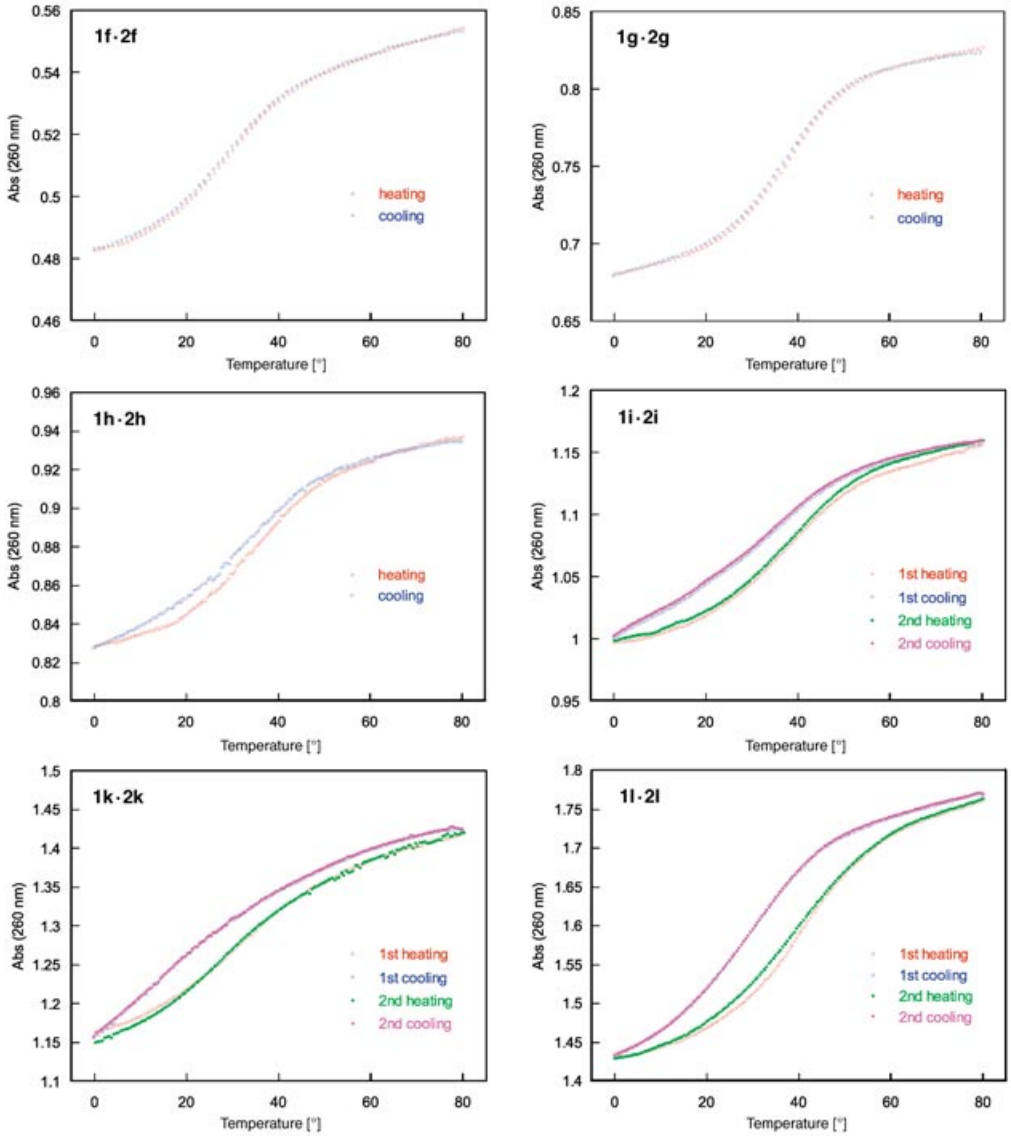

Fig. 2. *UV Melting curves of the duplexes* **1f**·**2f**, **1g**·**2g**, **1h**·**2h**, **1i**·**2i**, **1k**·**2k**, **1l**·**2l** (*Table 2*, *Entries 12–17*). Conditions: 2 μM duplex concentration, 150 mM NaCl, and 10 mM *Tris*·HCl (pH 7.4) in H_2O; heating and cooling rate: 0.5°/min.

pairs, however, stabilize the duplex more than would be expected from the sum of the individual contributions of the dangling residues. It can, thus, be concluded that the stabilization by terminally attached phenanthrene pairs is the result of a cooperative effect rather than of the sum of dangling-end contributions.

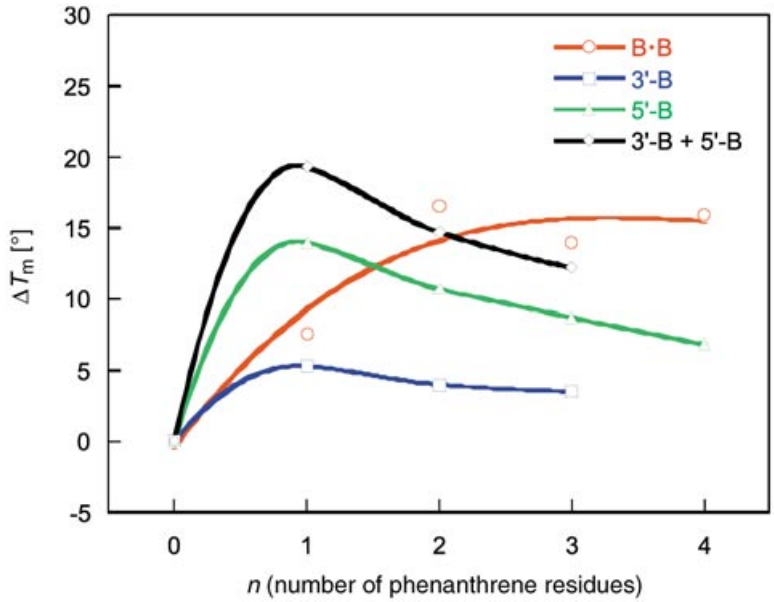

Fig. 3. *Plot of* ΔT_m *values against the number* n *of attached phenanthrene residues.* Curves show the effect of terminal phenanthrene pairs (red), 3′-dangling phenanthrene residues (blue), 5′-dangling phenanthrene residues (green), and the sum of 3′- and 5′-dangling phenanthrene residues (black).

2.5. *Gel Mobility Assays.* To obtain more information on the stability of DNAs with terminal phenanthrene stretches, we investigated the migration behavior of the corresponding duplexes under native conditions. Surprised by the large hysteretic effect and the low T_m values of duplexes **1k**·**2k** and **1l**·**2l** we further investigated the duplex stability by gel shift experiments. *Fig. 4* shows the mobility on polyacrylamide-gel electrophorese (PAGE) at room temperature of the six different hybrids **1f**·**2f**, **1g**·**2g**, **1h**·**2h**, **1i**·**2i**, **1k**·**2k**, and **1l**·**2l** in comparison with the nonmodified reference duplex **1r**·**2r** (see *Table 2*, *Entries 11–17*). After staining with ethidium bromide, all lanes exhibited one band, indicating the oligomers are migrating as pairs. The obvious gradual decrease in migration velocity, caused by each additional pair of phenanthrene residues, is due to the increase in molecular mass and thus well in agreement with the expectations.

The duplex **1l**·**2l**, composed of six nucleotide and six phenanthrene residues (*Table 2*, *Entry 17*) was further analyzed by temperature-dependent gel mobility assays. PAGEs were run at three different temperatures, 25, 50, and 70° under nondenaturing conditions (*Fig. 5*). At 25 and 50°, the two complementary strands **1l**·**2l** clearly migrate as one single band, corresponding to a duplex. At 70°, however, two bands corresponding to the two single strands are visible. Thus, the duplex **1l**·**2l** is stable up to a temperature of 50°. This does not correlate with the T_m values of 29.6 or 40.2° obtained from the UV transition curves (see *Table 2*, *Entry 17* and *Fig. 2*). Obviously, the transition observed in the UV melting curve does not arise from the melting of the whole duplex. Rather, that observed transition corresponds to the melting of the DNA

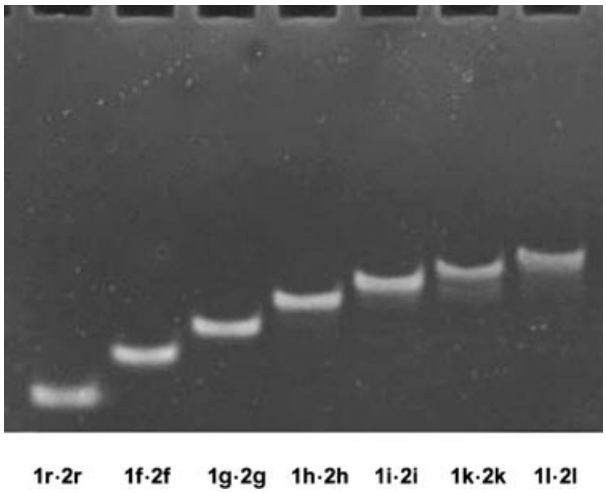

Fig. 4. *PAGE of phenanthrene-modified DNA duplexes.* The number of phenanthrene pairs attached to the DNA stem gradually increases from 0 to 6 (from left to right). Bands were visualized by staining with ethidium bromide.

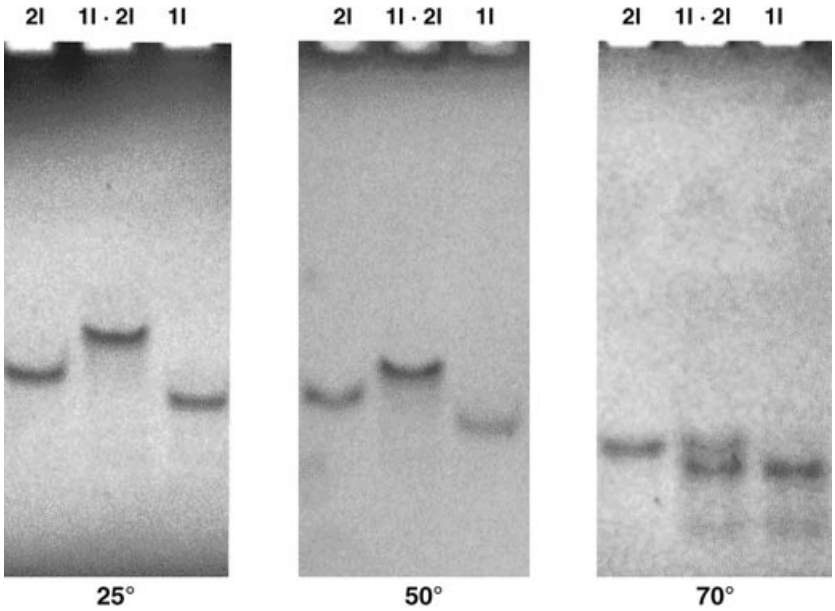

Fig. 5. *PAGE analysis of duplex* **1l**·**2l** *and the single strands* **1l** *and* **2l** *at different temperatures.* Bands were visualized under UV light.

part of the chimeric duplex. A second transition, *i.e.*, the denaturation of the phenanthrene part, occurs at higher temperature but is not observable by measurement of UV absorption, probably due to a lack of hyperchromicity.

2.6. *CD Spectroscopy of the Phenanthrene-Modified Duplexes. Fig. 6* shows the circular dichroism (CD) spectra of the duplexes **1a**·**2a**, **1b**·**2b**, **1c**·**2c**, **1d**·**2d**, **1e**·**2e** (*Table 1*, *Entries 1–5*) measured at 5°. All other conditions were identical to the thermal denaturation experiments. The spectra of all hybrids show a minimum CD effect in the range of 250 ± 10 nm and a maximum in the range of 275 ± 10 nm, which is very characteristic for B-form DNA. An intact B-form is, thus, maintained within the DNA parts of the different hybrids. In addition, a maximum CD effect is observed at 240–245 nm for the duplex **1c**·**2c** and – a very strong one – for duplex **1e**·**2e**. Both of these hybrids contain three phenanthrene units. This maximum is not observed for duplexes having only a single phenanthrene pair, and it is much more pronounced when the phenanthrene stretch is embedded within the DNA core rather than attached at the end of the DNA stem. This suggests that stretches of phenanthrene residues – although achiral building blocks by themselves – contribute to the secondary structure of the hybrid formed by the chimeric oligomers.

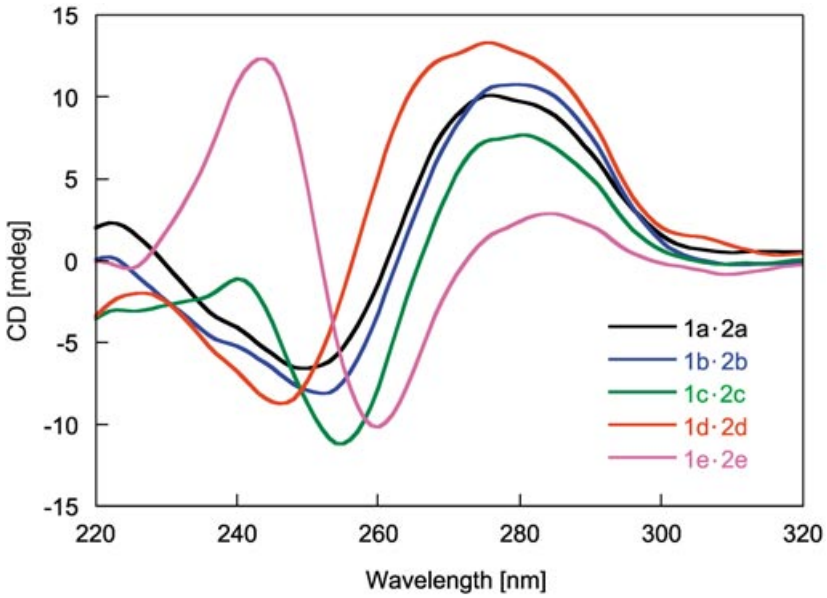

Fig. 6. *CD Spectra of the duplexes* **1a**·**2a**, **1b**·**2b**, **1c**·**2c**, **1d**·**2d**, *and* **1e**·**2e**. Conditions: 2 μM duplex concentration, 150 mM NaCl, and 10 mM *Tris*·HCl (pH 7.4) in H_2O; 5°.

2.7. *Model of a DNA Duplex Containing Terminal Phenanthrene Pairs.* A model of the **1g**·**2g** duplex, composed of six DNA base pairs and two phenanthrene pairs is shown in *Fig. 7*. The conformation represents a local-minimum structure obtained with Hyperchem starting from B-form DNA by using the *AMBER2* force-field. The following findings were taken into account: *i*) the DNA stem maintains an intact B-form; *ii*) phenanthrene units of the two strands contribute to hybrid stability through cooperative π-stacking interactions between the strands, and *iii*) despite the achiral nature of the building blocks, phenanthrene stretches contribute to the secondary

structure of the hybrid formed by the chimeric oligomers. Thus, the model illustrates the interstrand stacking of the phenanthrene residues on top of a B-form DNA. The top view (right part of *Fig. 7*) shows the arrangement of the phenanthrene residues along the helical axis. The phenanthrene residues are stacking in a zipper-like fashion on top of the bases of the DNA stem without disrupting its B-form structure.

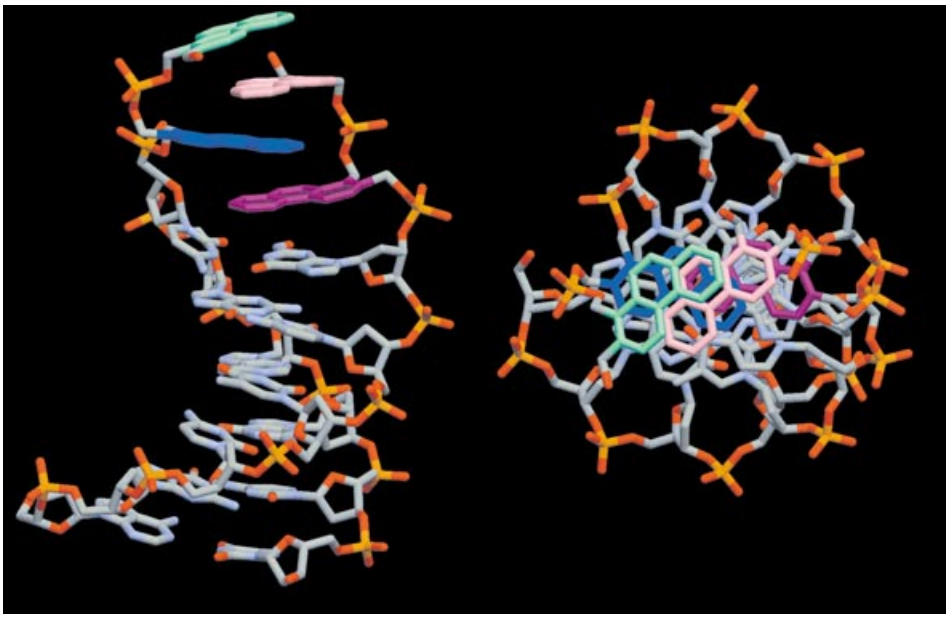

Fig. 7. *AMBER2-Minimized model of duplex* **1g**·**2g**. The four phenanthrene-1,2-dimethyl moieties are highlighted in non-CPK-colors. Left: view perpendicular to the helical axis; right: view along the helical axis.

3. Conclusions. – Phenanthrene-1,2-dimethanol was synthesized and evaluated as a nonnucleosidic, non-H-bonding DNA-base surrogate. The building block strongly disfavors duplex formation when placed at internal positions of a DNA stem. The destabilization is likely due to a bad geometric match of the two different stacking systems (*i.e.*, DNA and phenanthrene stretches). Terminal attachment of phenanthrene residues, however, leads to a substantial increase in stability. The stabilization is due to a cooperative interaction of the phenanthrene units of the two strands rather than to dangling-end effects. The DNA part of the chimeric hybrids maintains the common B-form structure. Chimeric oligomers containing a stretch of six phenanthrene residues show two separate transitions: one arising from the denaturation of the DNA stem (observable by a hyperchromic effect at 260 nm) and a second one from the denaturation of the phenanthrene part (observable by temperature-dependent gel mobility assays). Based on these findings, a model of the chimeric hybrids is proposed, in which the phenanthrene residues stack in a zipper-like way on top of the DNA base pairs without disrupting the B-form of the DNA stem.

Experimental Part

1. *General.* The *2-cyanoethyl diisopropylphosphoramidochloridite* was prepared as described in [23]. If not indicated otherwise, chemicals and solvents for reactions were purchased from *Fluka*, *Acros*, or *Aldrich* and were used without further purification. TLC: silica gel *SIL G-25 UV_{254}* glass plates (*Macherey-Nagel*); UV detection and/or dipping in a soln. of anisaldehyde/H_2SO_4/EtOH 1:1:18, followed by heating. Flash column chromatography (FC): silica gel *60* (63–32 μm, *Chemie Brunschwig AG*). CD Spectra: *Jasco J-715* spectropolarimeter with a 150-W Xe high-pressure lamp and a *Jasco PDF-350S-Peltier* unit, coupled with a *Colora K5* ultrathermostat, for the control of the temp. of the cell holder; temp. determination directly in the sample. ^{1}H- and ^{13}C-NMR: *Bruker AC-300*; δ values in ppm (solvent signals as internal references), J in Hz. ^{31}P-NMR: *Bruker AMX-400*; δ values in ppm (85% H_3PO_4 as external reference). ESI-MS: *VG-Platform* single-quadrupole ESI spectrometer; in m/z.

2. *Phosphoramidite Building Block* **1** *and Solid Support* **8**. *1-Ethenylnaphthalene* (**2**). After stirring a suspension of ^{t}BuOK (6.3 g, 56 mmol) and $MePPh_3Br$ (20 g, 56 mmol) in THF (200 ml) for 10 min at r.t., naphthalene-1-carboxaldehyde (6.0 g, 37 mmol) was added. The mixture was stirred for 60 min at r.t., then the reaction was quenched by adding 10% citric acid soln. in H_2O (200 ml) and, after evaporation of THF, the residue was extracted with hexane (3×). The org. phase was dried ($MgSO_4$) and evaporated and the residue adsorbed on SiO_2 (30 g). Purification by FC (SiO_2 20 g), hexane → hexane/AcOEt 9:1) gave **2** (5.5 g, 95%). Colorless oil. TLC (hexane/AcOEt 9:1): R_f 0.90.

Phenanthrene-1,2-dicarboxylic Acid Dimethyl Ester (**3**). A soln. of **2** (5.5 g, 35.7 mmol) and dimethyl ethynedicarboxylate (17.7 g, 125 mmol) in *o*-xylene (80 ml) was stirred for 3 h at 130°. All volatile compounds were evaporated, and the residue was adsorbed on SiO_2 (20 g). Purification by FC (SiO_2 30 g), hexane → hexane/AcOEt 6:4) gave **3** (3.4 g, 34%). Colorless solid. TLC (hexane/AcOEt 8:2): R_f 0.35. ^{1}H-NMR (300 MHz, $CDCl_3$): 3.99, 4.11 (2*s*, 2 Me); 7.68–7.74 (*m*, H–C(3), H–C(6), H–C(7)); 7.85 (*d*, J = 9.0, H–C(9)); 7.93 (*dd*, J = 2.5, 8.0, H–C(8)); 8.23 (*d*, J = 9.0, H–C(10)); 8.71 (*dd*, J = 2.1, 8.0, H–C(5)); 8.80 (*d*, J = 8.7, H–C(4)). ^{13}C-NMR (75 MHz, $CDCl_3$): 52.7, 53.0 (2*q*, Me); 121.31, 121.35, 124.0 (3*d*, arom. C); 125.1 (*s*, arom. C); 126.3, 127.4, 128.17 (3*d*, arom. C); 128.21 (*s*, arom. C); 128.2, 128.7, 129.1 (3*d*, arom. C); 129.4, 132.5, 133.3, 134.9 (4*s*, arom. C); 166.1, 169.8 (2*s*, C(O)). ESI-MS (pos.): 317.0783 ($C_{18}H_{14}O_4Na^+$; calc. 317.0789).

Phenanthrene-1,2-dimethanol (**4**). A soln. of **3** (2.2 g, 7.5 mmol) and MeOH (900 μl, 22 mmol) in THF (30 ml) was carefully treated with $LiBH_4$ (490 mg, 22 mmol) at 4°. After refluxing for 1 h, the mixture was cooled in an ice bath, and the reaction was quenched by the addition of H_2O (5 ml) followed by careful addition of 1N HCl (50 ml). The mixture was extracted with CH_2Cl_2 (3× 50 ml) and the org. phase dried ($MgSO_4$) and evaporated. The residue was suspended in AcOEt (20 ml) and the suspension refluxed for 30 min, diluted with hexane (10 ml), and cooled to r.t. The fine white crystals were filtered and washed with AcOEt/hexane 1:1: **4** (768 mg, 43%). TLC (hexane/AcOEt 1:1): R_f 0.15. ^{1}H-NMR (300 MHz, $CDCl_3$): 4.88, 5.12 (2*s*, CH_2OH); 7.47–7.59 (*m*, H–C(6), H–C(7)); 7.66 (*d*, J = 8.7, H–C(3)); 7.75 (*d*, J = 9.2, 1 arom. H); 7.81 (*dd*, J = 1.5, 8.5, H–C(8)); 8.16 (*d*, J = 9.4, 1 arom. H); 8.66 (*d*, J = 8.1, H–C(5)); 8.68 (*d*, J = 8.7, H–C(4)). ^{13}C-NMR (75 MHz, $CDCl_3$): 61.0, 66.1 (2*d*, CH_2OH); 127.5, 128.2, 128.8, 131.74, 131.78, 131.8, 131.9, 133.4 (8*d*, arom. C); 134.3, 135.2, 135.8, 136.1, 140.0, 144.3 (6*s*, arom. C). ESI-MS (pos.): 261.0884 ($C_{16}H_4O_2Na^+$; calc. 261.0891).

2-[[(4,4′-Dimethoxytrityl)oxy]methyl]phenanthrene-1-methanol (**5**) *and 1-[[(4,4′-dimethoxytrityl)oxy]-methyl]phenanthrene-2-methanol* (**6**). A soln. of **4** (610 mg, 2.5 mmol) in pyridine (10 ml) was treated with Et_3N (1.40 ml, 10 mmol) and $(MeO)_2TrCl$ (1.21 g, 3.6 mmol), stirred overnight at r.t., and then diluted with CH_2Cl_2 (50 ml) and 10% citric acid soln. in H_2O (50 ml). The mixture was extracted with CH_2Cl_2 (3×), the org. phase dried ($MgSO_4$) and evaporated, and the residue adsorbed on SiO_2 (4 g). Purification by two FCs SiO_2 (40 g); hexane → hexane/AcOEt 6:4; then SiO_2 (20 g); hexane/AcOEt 9:1 → hexane/AcOEt 8:2) gave **5** (585 mg, 42%) and **6** (110 mg, 8%).

Data of **5**: TLC (hexane/AcOEt 7:3): R_f 0.50. ^{1}H-NMR (300 MHz, $CDCl_3$): 2.75 (br. *s*, OH); 3.80 (*s*, MeO); 4.42 (*s*, ArCH_2C); 4.95 (*s*, CH_2OH); 6.85–6.91 (*m*, 4 arom. H); 7.23–7.36 (*m*, 3 arom. H); 7.43–7.46 (*m*, 4 arom. H); 7.51–7.69 (*m*, 5 arom. H); 7.84 (*d*, J = 9.3, H–C(9)); 7.91 (*dd*, J = 1.4, 7.6 H–C(8)); 8.22 (*d*, J = 9.3, H–C(10)); 8.69, 8.71 (2*d*, J = 8.5, 8.1, H–C(4), H–C(5)). ^{13}C-NMR (75 MHz, $CDCl_3$): 55.2 (*q*, Me); 58.4, 65.9 (2*d*, CH_2); 87.6 (*s*, Ar_3CO); 113.4, 122.6, 122.8, 123.0, 126.72, 126.75, 127.0, 127.8, 127.94, 128.01, 128.15, 128.5, 130.0 (13*d*, arom. C); 130.4, 130.7, 131.1, 131.6, 135.5, 135.8, 136.6, 144.7, 158.6 (9*s*, arom. C). ESI-MS (pos.): 563.2192 ($C_{37}H_{32}O_4Na^+$; calc. 563.2198).

Data of **6**: TLC (hexane/AcOEt 1:1): R_f 0.25. ^{1}H-NMR (300 MHz, $CDCl_3$): 2.74 (br. *s*, OH), 3.71 (*s*, MeO); 4.58, 4.61 (2*s*, ArCH_2O); 6.77–6.82 (*m*, 4 arom. H); 7.15–7.27 (*m*, 4 arom. H); 7.37–7.64 (*m*, 9 arom. H); 7.74–7.82 (*m*, 2 arom. H); 8.60–8.65 (*m*, H–C(4), H–C(5)). ^{13}C-NMR (75 MHz, $CDCl_3$): 55.3 (*q*, MeO); 59.3,

63.9 (2*d*, CH_2); 87.3 (*s*, Ar_3CO); 113.4, 122.9, 123.1, 123.4, 126.7, 127.0, 127.2, 128.0, 128.2, 128.3, 128.5, 130.2, 130.41 (13*d*, arom. C); 130.45, 131.1, 131.4, 132.6, 135.7, 139.5, 144.6, 158.7 (8*s*, arom. C). ESI-MS (pos.): 563.2213 ($C_{37}H_{32}O_4Na^+$; calc. 563.2198).

Chloroacetic Acid [2-(Hydroxymethyl)phenanthren-1-yl]methyl Ester (**7**). A soln. of **5** (100 mg, 0.186 mmol), collidine (40 mg, 0.33 mmol), and chloroacetic anhydride (38 mg, 0.22 mmol) in CH_2Cl_2 (0.4 ml) was stirred for 15 min at r.t. The reaction was quenched by the addition of 10% citric acid soln. in H_2O (50 ml), the mixture extracted with CH_2Cl_2 (3 × 50 ml), and the org. phase dried ($MgSO_4$) and evaporated. The crude was dissolved in HCOOH/THF/EtOH 50 : 35 : 15 (*v/v*; 6 ml), and the soln. was stirred for 20 min at r.t. After addition of 1M NH_4Cl in H_2O (10 ml), THF and EtOH were evaporated. The residue was extracted with CH_2Cl_2 (3×), the org. phase dried ($MgSO_4$) and evaporated, and the crude adsorbed on SiO_2 (300 mg). Purification by FC (SiO_2 (2 g); hexane → hexane/AcOEt 8 : 2) gave **7** (18 mg, 32%). White solid. TLC (hexane/AcOEt 7 : 3): R_f 0.15. ^{1}H-NMR (400 MHz, $CDCl_3$): 4.06 (*s*, CH_2Cl); 5.05 (*d*, *J* = 5.6, CH_2OH); 5.92 (*s*, $ArCH_2O$); 7.62 – 7.71 (*m*, H–C(6), H–C(7)); 7.74 (*d*, *J* = 8.6, H–C(3)); 7.86, 8.04 (2*d*, *J* = 9.3, H–C(9), H–C(10)); 7.92 (*dd*, *J* = 1.1, 7.4, H–C(8)); 8.70 (*d*, *J* = 8.2, H–C(5)); 8.77 (*d*, *J* = 6.6, H–C(4)). NOE (irr. Signal → affected signals): 5.05 (CH_2OH) → 2.32 (*d*, OH; 1.6%), 5.92 (*d*, $ArCH_2OC$; 3.0%), and 7.74 (*d*, H–C(3); 3.7%); 5.92 ($ArCH_2OC$) → 5.05 (*d*, CH_2OH; 4.5%) and 8.04 (*d*, H–C(10); 8.4%); 8.04 (H–C(10)) → 5.92 (*d*, $ArCH_2OC$; 8.7%), 7.86 (*d*, H–C(9); 2.4%), and 7.92 (neg. *d*, artefact), but no effect at 8.77 (*d*, *J* = 6.6, H–C(4)). ^{13}C-NMR (75 MHz, (D_6)MSO): 46.4, 65.8, 66.1 (3*d*, CH_2); 127.7, 128.2, 129.3, 131.8, 132.1, 132.3, 132.9 (7*d*, arom. C); 133.4 (*s*, arom. C); 133.5 (*d*, arom. C); 134.4, 135.0, 136.0, 136.1, 146.1 (5*s*, arom. C); 172.6 (*s*, C=O). ESI-MS (pos.): 314.0710 ($C_{18}H_{15}ClO_3^+$; calc. 314.0710).

{2-{[(4,4′-Dimethoxytrityl)oxy]methyl}phenanthren-1-yl}methyl Diisopropylphosphoramidite (**1**). A soln. of **5** (340 mg, 0.6 mmol) and ^{i}Pr$_2$NEt (270 µl, 1.6 mmol) in CH_2Cl_2 (4 ml) was treated with 2-cyanoethyl diisopropylphosphoramidochloridite (200 mg, 0.8 mmol), stirred for 2 h at r.t., and then purified by FC SiO_2 (6 g), hexane (+2% Et_3N) → hexane/AcOEt 7 : 3 (+2% Et_3N): **1** (390 mg, 88%). White foam. TLC (hexane/AcOEt 7 : 3): R_f 0.65. ^{1}H-NMR (300 MHz, $CDCl_3$): 0.92, 1.05 (2*d*, *J* = 6.8, $(Me_2CH)_2N$); 2.35 (*dt*, *J* = 3.2, 1.1, OCH_2CH_2CN); 3.47 – 3.59 (*m*, $(Me_2CH)_2N$, OCH_2CH_2CN); 3.73 (*s*, MeO); 4.51 (*s*, $ArCH_2OC$); 4.97 – 5.15 (*m*, $ArCH_2OP$); 6.84 – 6.89 (*m*, 4 arom. H); 7.21 – 7.36 (*m*, 3 arom. H); 7.42 – 7.47 (*m*, 4 arom. H); 7.53 – 7.69 (*m*, 4 arom. H); 7.80 (*d*, *J* = 9.2, H–C(9)); 7.90 (*d*, *J* = 8.5, H–C(8)); 8.15 (*d*, *J* = 9.2, H–C(10)); 8.72, 8.75 (2*d*, *J* = 9.0, 8.8, H–C(4), H–C(5)). ^{13}C-NMR (75 MHz, $CDCl_3$): 20.1 (*t*, *J*(C,P) = 6.8, CH_2CN); 24.50, 24.60, (2*q*, *J*(C,P) = 7, $(Me_2CH)_2N$); 43.2 (*d*, *J*(C,P) = 12, $(Me_2CH)_2N$); 55.2 (*q*, MeO); 58.4, 58.8 (2*d*, *J*(C,P) = 20, 17, $ArCH_2OP$, $POCH_2CH_2CN$); 64.0 (*d*, $ArCH_2OC$); 86.8 (*s*, Ar_3CO); 113.2 (*d*, arom. C); 117.6 (*s*, CN); 122.7, 123.1, 123.31, 123.34, 126.5, 126.6, 126.7, 126.8, 127.2, 127.9, 128.3, 128.4, 130.2 (13*d*, arom. C); 130.4, 131.1, 131.5, 132.5, 132.6, 136.2, 136.3, 145.1, 158.5 (9*s*, arom. C). ^{31}P-NMR (121 MHz, $CDCl_3$): 149.2. ESI-MS (pos.): 763.3259 ($C_{46}H_{49}N_2O_5PNa^+$; calc. 763.3276).

Solid support **8** (=*{4-{2-[(Controlled-pore-glass)amino]-2-oxoethoxy}phenoxy}acetic Acid {2-{[(4,4′-Dimethoxytrityl)oxy]methyl}penanthren-1-yl}methyl Ester*). A soln. of **5** (116 mg, 0.21 mmol), [1,4-phenylenebis(oxy)]bis[acetic acid] (97 mg, 0.43 mmol), DMAP (5 mg, 0.04 mmol), and ^{i}Pr$_2$NEt (185 µl, 1.1 mmol) in pyridine (2 ml) was treated with BOP (190 mg, 0.43 mmol) and kept for 30 min at r.t. The mixture was diluted with CH_2Cl_2 (20 ml) and 10% citric acid soln. in H_2O (30 ml). After extraction with CH_2Cl_2 (3 × 20 ml), the org. phase was washed with sat. aq. $NaHCO_3$ soln., dried ($MgSO_4$) and evaporated and the crude purified by FC (SiO_2 (1 g), CH_2Cl_2 (+2% Et_3N) → CH_2Cl_2/MeOH 19 : 1 (+2% Et_3N)) to give the intermediate as Et_3NH^+ salt. ^{1}H-NMR (300 MHz, $CDCl_3$): 1.25 (*t*, *J* = 7.4, $(Me_2CH_2)_3N$); 2.99 (*q*, *J* = 7.4, $(Me_2CH_2)_3N$); 3.69 (*s*, MeO); 4.32, 4.34, 4.35, 5.54 (4*s*, CH_2); 6.62 – 6.79 (*m*, 8 arom. H); 7.13 – 7.78 (*m*, 15 arom. H); 8.61 – 8.69 (*m*, H–C(4), H–C(5)).

The intermediate (25 mg, 0.03 mmol) was dissolved in a suspension of (long-chain-alkyl)amino controlled-pore glass (LCAA-CGP; 500 mg), ^{i}Pr$_2$NEt (60 µl, 0.36 mmol), and BOP (13 mg, 0.03 mmol) in MeCN and shaken for 20 h at r.t. After filtration, the solid phase was washed with MeCN and CH_2Cl_2, suspended in pyridine (1.5 ml) and Ac_2O (0.5 ml), and shaken for 2 h at r.t. The solid was filtered and washed with DMF and CH_2Cl_2. Loading density (trityl monitoring): 26 µmol/g.

3. *Synthesis and Purification of Oligonucleotides.* Oligonucleotides were synthesized on a *392-DNA/RNA* synthesizer (*Applied Biosystems*) according to the phosphoramidite chemistry [24][25]. The deoxynucleoside phosphoramidites were from *ChemGenes* (Ashland, MA). Oligonucleotides were prepared by the standard synthetic procedure ('trityl-off' mode), by using 1.1M *tert*-butyl hydroperoxide (in hexane/1,2-dichlorethane 1 : 4) as the oxidant. For the phenanthrenylmethyl phosphoramidite **1**, used as a 0.1M soln. in 1,2-dichloroethane, the coupling time was increased to 50 s in the presence of 0.25M 5-(benzylthio)-1*H*-tetrazole in MeCN as activator. Cleavage from the solid support and final deprotection was achieved by treatment with 30% NH_4OH soln.

overnight at 55°. The nonmodified oligonucleotides were purified anion by exchange HPLC, (*Source 15Q 4.6/100 PE* (*Pharmacia*); eluent *A*, 20 mM Na_2HPO_4 (pH 11.5); eluent *B*, 20 mM NaH_2PO_4, 2M NaCl (pH 11.5)). The modified oligonucleotides were purified by reversed-phase HPLC (*LiChrospher 100 RP-18* (5 μm; *Merck*); eluent *A*, 0.1M (Et_3NH)OAc in H_2O (pH 7.0); eluent *B*, MeCN; elution at 50°). The purified oligonucleotides were desalted with *Sep-Pak* cartridges (*Waters*, Milford, USA; eluent A, 0.1M (Et_3NH)OAc; eluent *B*, H_2O/MeCN 1:1). The molecular masses of the purified oligonucleotides were determined by ESI-MS. The data of all oligomers are summarized In *Table 3:*

Table 3. *ESI-MS and Other Data of the Synthesized Oligomers*

	Sequence[a])	A.u. [*OD*]	ε [cm^{-1} M^{-1}]	MS [*m/z*][b])	
				calc.	found
1a	5′ AGC TCG GTC ATC 3′	15	122300	3621	3620
2a	3′ TCG AGC CAG TAG 5′	27	132900	3670	3670
1b	5′ AGC TCG GTC AT**B** 1”	66	157900	3632	3631
2b	3′ TCG AGC CAG TA**B** 2”	20	164200	3641	3640
1c	5′ AGC TCG GTC **BBB** 1”	55	219600	3616	3615
2c	3′ TCG AGC CAG **BBB** 2”	22	225900	3624	3624
1d	5′ AGC TCG **B**TC ATC 3′	40	153600	3592	3591
2d	3′ TCG AGC **B**AG TAG 5′	24	168500	3681	3681
1e	5′ AGC T**BB B**TC ATC 3′	38	220500	3575	3574
2e	3′ TCG A**BB B**AG TAG 5′	31	235400	3664	3662
1r	5′ AGC TCG 3′	29	62500	1792	1793
2r	3′ TCG AGC 5′	31	62500	1792	1792
1f	5′ AGC TCG **B** 1″	99	105500	2093	2093
2f	3′ TCG AGC **B** 2″	27	105500	2093	2093
1g	5′ AGC TCG **BB** 1″	51	148500	2393	2393
2g	3′ TCG AGC **BB** 2″	40	148500	2393	2393
1h	5′ AGC TCG **BBB** 1″	55	191500	2693	2694
2h	3′ TCG AGC **BBB** 2″	27	191500	2693	2693
1i	5′ AGC TCG **BBB B** 1″	67	234500	2993	2993
2i	3′ TCG AGC **BBB B** 2″	36	234500	2993	2993
1k	5′ AGC TCG **BBB BB** 1″	25	277500	3293	3294
2k	3′ TCG AGC **BBB BB** 2″	34	277500	3293	3293
1l	5′ AGC TCG **BBB BBB** 1″	35	320500	3593	3594
2l	3′ TCG AGC **BBB BBB** 2″	31	320500	3593	3594

[a]) **B** is the nonnucleosidic phenanthrene unit; 1″ or 2″ denotes linkage to CH_2O at C(1) or C(2), respectively of the phenanthrene unit. [b]) Calculated for $[M-H]^-$.

4. *Thermal Denaturation Experiments.* All experiments were carried out under the following conditions: 2.0 μM oligonucleotide concentration (each strand), 10 mM *Tris*·HCl buffer (pH 7.4), and 150 mM NaCl. UV Melting Curves: *Varian Cary-3e*-UV/VIS spectrophotometer equipped with a *Peltier*-block temperature controller. The *Varian WinUV* software were utilized to determine the melting curves at 260 nm, a heating-cooling-heating cycle in the temp. range of 0–80° was applied with a temp. gradient of 0.5°/min. To avoid H_2O condensation on the UV cells at $<<20°$, the cell compartment was flushed with N_2. Data were collected and analyzed with *Kaleidagraph*® software from ©*Synergy Software*. T_m Values were determined as the maximum of the first derivative of the melting curve.

5. *PAGE Experiments. Equipment*. *Mini-Protean III* (*Bio-Rad*); *EPS-3500 XL* (*Pharmacia Biotech*) power supply. Buffer: 5 × TBE (=450 mM *Tris* 450 mM boric acid 10 mM EDTA).

Preparation of 16% Gels. An aq. soln. of 40% acrylamide/bisacrylamide 19:1 (4 ml) was diluted with 5 × TBE (2 ml) and H_2O (4 ml). After degassing the acrylamide soln., a soln. of 10% APS (ammonium persulfate) in H_2O (20 μl) and TMEDA (tetramethylethylenediamine; 20 μl) was added, and the gel was allowed to polymerize within 1 h.

Running the Gels. Loading of oligonucleotide (0.1 *OD*) in formamide/H_2O 1:1 (6 µl) per well. Elution buffer: 1 × TBE. Electrophoresis was carried out at 150–200 V for 20 min at 25, 50 or 70°. The bands of the gels were directly photographed under UV light or stained with ethidium bromide.

6. *Modelling.* The structure of the duplex **1g**·**2g** (see *Fig. 7*) was minimized by using the AMBER2 force field (Hyperchem 7.0, *Hypercube*, Waterloo, Ontario).

REFERENCES

[1] J. Wengel, *Org. Biomol. Chem.* **2004**, *2*, 277.
[2] C. A. Hunter, K. R. Lawson, J. Perkins, C. J. Urch, *J. Chem. Soc., Perkin Trans. 2* **2001**, 651.
[3] I. Singh, W. Hecker, A. K. Prasad, S. P. A. Virinder, O. Seitz, *Chem. Commun.* **2002**, 500.
[4] M. Berger, A. K. Ogawa, D. L. McMinn, Y. Q. Wu, P. G. Schultz, F. E. Romesberg, *Angew. Chem., Int. Ed.* **2000**, *39*, 2940.
[5] D. L. McMinn, A. K. Ogawa, Y. Q. Wu, J. Q. Liu, P. G. Schultz, F. E. Romesberg, *J. Am. Chem. Soc.* **1999**, *121*, 11585.
[6] R. X. F. Ren, N. C. Chaudhuri, P. L. Paris, S. Rumney, E. T. Kool, *J. Am. Chem. Soc.* **1996**, *118*, 7671.
[7] J. M. Gao, C. Strassler, D. Tahmassebi, E. T. Kool, *J. Am. Chem. Soc.* **2002**, *124*, 11590.
[8] C. Brotschi, A. Haberli, C. J. Leumann, *Angew. Chem., Int. Ed.* **2001**, *40*, 3012.
[9] G. Mathis, J. Hunziker, *Angew. Chem., Int. Ed.* **2002**, *41*, 3203.
[10] E. T. Kool, J. C. Morales, K. M. Guckian, *Angew. Chem., Int. Ed.* **2000**, *39*, 990.
[11] S. Bommarito, N. Peyret, J. SantaLucia, *Nucl. Acids. Res.* **2000**, *28*, 1929.
[12] K. M. Guckian, B. A. Schweitzer, R. X. F. Ren, C. J. Sheils, P. L. Paris, D. C. Tahmassebi, E. T. Kool, *J. Am. Chem. Soc.* **1996**, *118*, 8182.
[13] A. A. Mokhir, C. Richert, *Nucleic Acids Res.* **2000**, *28*, 4254.
[14] J. Tuma, W. H. Connors, D. H. Stitelman, C. Richert, *J. Am. Chem. Soc.* **2002**, *124*, 4236.
[15] J. Michel, K. Bathany, J. M. Schmitter, J. P. Monti, S. Moreau, *Tetrahedron* **2002**, *58*, 7975.
[16] S. M. Langenegger, R. Häner, *Helv. Chim. Acta* **2002**, *85*, 3414.
[17] S. M. Langenegger, R. Häner, *Chem. Biodiv.* **2004**, *1*, 259.
[18] C. B. Nielsen, M. Petersen, E. B. Pedersen, P. E. Hansen, U. B. Christensen, *Bioconjug. Chem.* **2004**, *15*, 260.
[19] U. B. Christensen, M. Wamberg, F. A. El Essawy, A. Ismail, C. B. Nielsen, V. V. Filichev, C. H. Jessen, M. Petersen, E. B. Pedersen, *Nucleosides Nucleotides Nucleic Acids* **2004**, *23*, 207.
[20] C. M. Chan, *Synth. Commun.* **1989**, *19*, 1981.
[21] K. Soai, A. Ookawa, *J. Org. Chem.* **1986**, *51*, 4000.
[22] R. T. Pon, S. Y. Yu, *Nucleic Acids Res.* **1997,** *25*, 3629–3635.
[23] M. V. Rao, C. B. Reese, V. Schehlmann, P. S. Yu, *J. Chem. Soc., Perkin Trans.1* **1993**, 43.
[24] S. L. Beaucage, M. H. Caruthers, *Tetrahedron Lett.* **1981**, *22*, 1859.
[25] N. D. Sinha, J. Biernat, J. McManus, H. Koster, *Nucleic Acids Res.* **1984**, *12*, 4539.

Received July 16, 2004